

## Birefringent cadmium–telluride-based metamaterial

M. L. Markham, J. J. Baumberg, and D. C. Smith<sup>a)</sup>

*School of Physics and Astronomy, University of Southampton, Highfield, Southampton SO17 1BJ, United Kingdom*

X. Li, T. Gabriel, G. S. Attard, and I. Nandhakumar

*School of Chemistry, University of Southampton, Highfield, Southampton SO17 1BJ, United Kingdom*

(Received 28 June 2004; accepted 2 November 2004; published online 27 December 2004)

A CdTe-based optical metamaterial, with large induced optical birefringence (4%), has been produced and its optical properties fully characterized and modeled over the spectral range 1500–450 nm. This metamaterial, which is related to mesoporous silica, is made using electrochemical deposition in the presence of a lyotropic liquid crystal template. This process produces a stoichiometric CdTe film containing a hexagonal array of  $\sim 4.2$  nm cylindrical pores with interpore separation  $\sim 6.5$  nm. A model of the dielectric properties of the films indicates that their birefringence can be entirely attributed to the film's nanoporosity. © 2005 American Institute of Physics. [DOI: 10.1063/1.1844035]

Three-dimensional nanostructuring of materials to produce metamaterials with innovative and optimized functional properties is a developing field which is already showing great promise. The most mature branch of this field is that of metamaterials with engineered electromagnetic properties. The most radical examples of these metamaterials are negative refractive index materials<sup>1</sup> and photonic crystals.<sup>2</sup> Metamaterials in which the electronic properties are controlled are less common, however the potential in this area is clearly demonstrated by nanocrystal superlattices involving the intimate combination of magnetic and semiconducting materials.<sup>3</sup>

The complexity and characteristic length scales associated with many metamaterials means that self-assembly techniques are an ideal method for producing them. One particularly promising route for this is the use of lyotropic liquid crystal templates which are cast into solid form using sol-gel or electrochemical deposition.<sup>4</sup> Powdered mesoporous silica and titania produced in this way have been known for some time and are commercially exploited as high surface area substrates for catalysis. For most optical and electronic applications, however, films or monoliths of these materials are required. These have already been used in a number of different applications including: low dielectric constant materials for transistors and optical coatings, supercapacitors,<sup>4,5</sup> and to produce hybrid polymer/titania solar cells.<sup>6</sup>

Although liquid crystal templated films<sup>7</sup> were first produced in 1995 the number of materials from which they have been produced is so far quite limited. In particular, of all the possible semiconductors, only the elemental semiconductors Te,<sup>8</sup> Se,<sup>9</sup> and the oxide semiconductors Cu<sub>2</sub>O and ZnO<sup>10</sup> have been templated. Cadmium–telluride is an ideal candidate as its band gap makes it well suited to photovoltaic devices and high quality CdTe can be produced electrochemically.<sup>11</sup> Liquid crystal templated CdTe should be an extremely interesting metamaterial with the nanostructuring allowing control of the electronic band structure, lattice vibrations, and charge carrier dynamics. In addition the introduction of a hexagonal array of parallel pores using an H<sub>2</sub>O

liquid crystal template (Fig. 1) will introduce strong form birefringence<sup>12</sup> into this normally nonbirefringent material. This birefringence opens up applications such as polarization-sensitive photoabsorption and phase-matched nonlinear optical components. In this letter we describe the production of high quality films of mesoporous CdTe and their characterization as optical metamaterials.

The films were fabricated using a standard potentiostatic electrochemical method with a three-electrode setup.<sup>8,13</sup> The plating mixture used consists of the deposition salts dissolved in sulphuric acid (0.15 M CdSO<sub>4</sub> and 0.005 M TeO<sub>2</sub>, 2 M H<sub>2</sub>SO<sub>4</sub>) and a commercial nonionic surfactant, C<sub>16</sub>EO<sub>8</sub> (50% by weight of the final mixture). The CdTe was deposited onto a 250-nm-thick gold on glass substrate, area  $\sim 1$  cm<sup>2</sup>, using a platinum gauze counter electrode and saturated calomel reference electrode (SCE). The films were deposited at room temperature for between 5 and 15 h giving films of thickness 100–350 nm. In order to improve the alignment of the liquid crystal, the deposition cell was sealed, to prevent water loss, and heated to a temperature (4 °C) above the isotropic point (at 63 °C) and then cooled at a rate of 0.2 °C/min. After deposition the surfac-

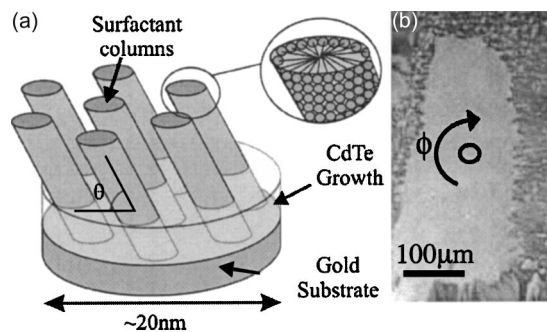


FIG. 1. (a) Representation of liquid crystal template at the surface of a gold electrode. Electrodeposition occurs from the aqueous phase surrounding the surfactant columns producing CdTe containing a hexagonal array of pores. (b) CdTe film viewed through crossed polarizers showing a large birefringent domain. Polarized micro-reflectance spectra were measured as a function of the rotation of the sample,  $\phi$ . The circle indicates the size of the region measured.

<sup>a)</sup>Electronic mail: dsmith@phys.soton.ac.uk

tant was removed by soaking in de-ionized water for at least 24 h.

The chemical composition and crystalline form of the films were characterized by energy dispersive x-ray analysis and x-ray diffraction (XRD). The films were found to be of uniform composition across the whole of the sample to within the sensitivity of the energy dispersive x-ray analysis measurements. It is possible to vary the measured composition of Cd to Te in the films over the range 27%/73% to 63%/37% by controlling the deposition potential from  $-0.5$  to  $-0.7$  V vs SCE. Stoichiometric films were produced in the range  $-0.54$  to  $-0.65$  V, with a standard deposition being performed at a potential of  $-0.58$  V. It was determined by monitoring the quasi-rest potential and resistive potential drop during test depositions that the deposition potential did not need to be adjusted during growth in order to maintain a stoichiometric composition.<sup>14</sup> All the diffraction peaks observed in wide angle XRD from stoichiometric films can be attributed to CdTe and the substrate. Interpreting the width of the diffraction peaks using the Debye–Sherrer (DS) formula gives grain sizes of 27 nm. This number should be taken as a lower limit as nearly all the atoms in these materials are at surfaces.

The nanostructuring of the films was determined using low angle XRD and transmission electron microscopy (TEM). The low angle XRD ( $\text{Cu } K\alpha$ ) typically only showed the  $d_{100}$  diffraction peak from the hexagonal array of pores. The lack of higher order peaks is expected from the pores form factor. The period obtained from the low angle XRD is  $6 \pm 1$  nm and the translational order length scale determined from the DS formula is 24 nm. TEM was performed on material scraped from films. The TEM pictures clearly show a hexagonal arrangement of pores with pore separation  $7 \pm 0.5$  nm.<sup>13</sup>

When viewed through crossed polarizers (Fig. 1), the samples show similar texturing to that of the lyotropic liquid crystal template with some large domains, of the order of  $1 \text{ mm}^2$ . A number of techniques<sup>15–17</sup> exist to produce alignment of lyotropic liquid crystals over large areas and with some effort it should be possible to produce single domain samples of areas greater than  $1 \text{ cm}^2$ . Films produced electrochemically on the same substrates without the liquid crystal template show no observable birefringence.

The “normal incidence” reflection spectra [Fig. 2(a)] of single domains (Fig. 1) of a number of different samples were measured using micro-spectroscopy with linearly polarized white light illumination and polarization insensitive detection. The sample was rotated about a vector perpendicular to the film through the measurement point. The spectra were normalized against a  $\text{SiO}_2$ -protected aluminum mirror. The reflectivity of the sample at specific wavelengths showed the expected sinusoidal variation with angle [Fig. 2(c)]. These measurements were used to determine the principal directions and their reflectance spectra.

The reflectance spectra show clear interference fringes which together with the visual observation of “mirror like” surfaces indicate the extremely flat surfaces of the films. Measurements on films produced with a range of different chemical compositions clearly indicate the difference between stoichiometric and nonstoichiometric films with the latter having considerable absorption at energies beneath the bulk CdTe band gap. The reflection spectrum of stoichiometric films have an inflection point at 820 nm, just higher in

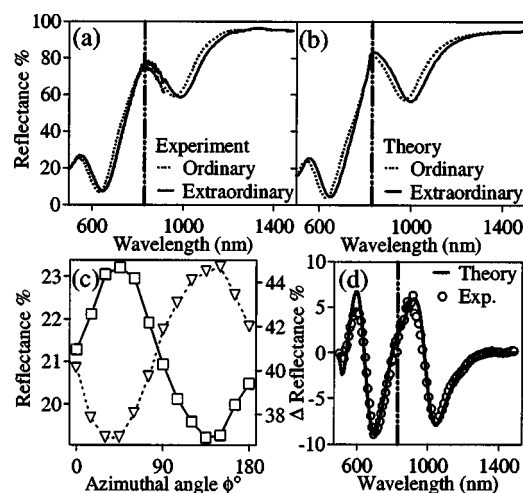


FIG. 2. (a) Measured reflectance spectra for light polarized parallel to the ordinary and extraordinary directions. (b) Theoretical predictions of spectra in (a). (c) Reflectance at 577 nm (squares, left axis) and 722 nm (triangles, right axis) as a function of the sample rotation  $\phi$ . (d) Comparison of measured and predicted difference between ordinary and extraordinary reflectance spectra. Vertical lines on (a), (b), and (d) indicate CdTe room temperature bandgap at 830 nm.

energy than the band gap of bulk CdTe, at 830 nm, which we attribute to the onset of absorption within the thin films. The slight blueshift in the absorption edge of the mesoporous material relative to bulk may be due to quantum confinement. However, confirmation of this will require further experimental investigations. A comparison of the reflectance spectra for the two principal directions shows a clear wavelength shift of the fringes as expected for an anisotropic material, with a birefringence of 4.3% for light traveling parallel to the film normal. This figure varies from domain to domain in the range 4.3% to 1.7%. Thus this CdTe metamaterial has birefringence in excess of that of KDP and approximately six times greater than quartz.<sup>18</sup>

In order to better quantify our measurements and determine if the observed birefringence could be explained solely by the nanostructuring of the films we have modeled the dielectric response expected for a mesoporous material in the long wavelength limit. The dielectric coefficient for light polarized parallel to the cylindrical holes is given trivially by the volume weighted average of the dielectric coefficients of CdTe and air;  $\epsilon_{\parallel} = f\epsilon_{\text{CdTe}} + (1-f)$  where  $f$  is the volume fraction of CdTe. For light polarized perpendicular to the cylindrical pores the result is far from trivial with a simple analytic formula only being available for pores whose diameter is much smaller than their separation,<sup>19,20</sup> the so called dilute limit. We have therefore modeled the perpendicular dielectric coefficient using two conceptually different models; direct numerical solution of Laplace’s equation using a finite difference scheme<sup>21</sup> and a Boundary Integral model<sup>22</sup> which has been solved analytically and numerically. The three solutions obtained are in full agreement that the dilute limit formula applies for a hexagonal arrangement of cylinders even if those cylinders are basically touching, i.e.,  $\epsilon_{\perp} = 1 + 2f(\epsilon_{\text{CdTe}} - 1) / (2 + (1-f)(\epsilon_{\text{CdTe}} - 1))$ . From the modeling, it is clear that this is due to the high symmetry arrangement of the cylinders in a hexagonal lattice and the same models applied to a rectangular lattice *do not* give the dilute limit.

Reflectance spectra (Fig. 2) are calculated from the modeled ordinary,  $n^o = \sqrt{\epsilon_{\perp}}$ , and extraordinary,  $n^e$

$= \sqrt{\epsilon_{\perp} \epsilon_{\parallel} / (\epsilon_{\perp} \cos^2 \theta + \epsilon_{\parallel} \sin^2 \theta)}$ , refractive indexes for normally incident light using a standard transmission matrix approach.<sup>23</sup> Not counting the separately determined bulk CdTe<sup>24</sup> and Au dielectric coefficients,<sup>25</sup> the fit contains three free parameters; the volume fraction of CdTe, which controls the fringe modulation depth, the thickness of the film, which controls the spectral position of the fringe maxima and minima, and the angle of the pores relative to the film normal  $\theta$ , which controls the birefringence. As can be seen in Fig. 2 the agreement between theory and experiments is extremely good. The fitting strongly constrains the fitting parameters. The sample thickness obtained from the best fit is  $317 \pm 5$  nm. The best fit volume fraction,  $0.63 \pm 0.07$ , corresponds to  $4.2 \pm 0.4$  nm-diameter pores for an interpore distance of 6.5 nm, which is well within the limits which can be placed on this parameter from the TEM data. As varying the pore angle,  $\theta$ , allows the predicted birefringence to vary from zero for parallel alignment to a maximum for perpendicular alignment it is possible to fit the full range of birefringences observed for different domains using this parameter alone. The range of best fit angles obtained,  $40$ – $17^\circ$ , is quite reasonable and hard to verify independently.

In conclusion we have produced a CdTe based metamaterial, containing a hexagonal array of  $\sim 4$  nm pores with separation  $\sim 6.5$  nm. This metamaterial has strong optical birefringence at energies above and below the band gap energy. The optical properties of films have been modeled using first principles electromagnetic simulations and have been shown to be entirely explicable in terms of the nanoporosity within the films.

This research was supported by EPSRC GR/S02662, GR/R54194, GR/S49162, and Merck Ltd. D.C.S. would like to thank EPSRC for an Advanced Fellowship GR/A11595.

<sup>1</sup>T. J. Yen, W. J. Padilla, N. Fang, D. C. Vier, D. R. Smith, J. B. Pendry, D. N. Basov, and X. Zhang, *Science* **303**, 1494 (2004).

- <sup>2</sup>C. M. Soukoulis, *Nanotechnology* **13**, 420 (2002).  
<sup>3</sup>F. X. Redl, K. S. Cho, C. B. Murray, and S. O'Brien, *Nature (London)* **423**, 968 (2003).  
<sup>4</sup>G. S. Attard, P. N. Bartlett, N. R. B. Coleman, J. M. Elliott, J. R. Owen, and J. H. Wang, *Science* **278**, 838 (1997).  
<sup>5</sup>P. A. Nelson and J. R. Owen, *J. Electrochem. Soc.* **150**, A1313 (2003).  
<sup>6</sup>K. M. Coakley and M. D. McGehee, *Appl. Phys. Lett.* **83**, 3380 (2003).  
<sup>7</sup>G. S. Attard, J. C. Glyde, and C. G. Goltner, *Nature (London)* **378**, 366 (1995).  
<sup>8</sup>T. Gabriel, I. S. Nandhakumar, and G. S. Attard, *Electrochem. Commun.* **4**, 610 (2002).  
<sup>9</sup>I. Nandhakumar, J. M. Elliott, and G. S. Attard, *Chem. Mater.* **13**, 3840 (2001).  
<sup>10</sup>H. M. Luo, J. F. Zhang, and Y. S. Yan, *Chem. Mater.* **15**, 3769 (2003).  
<sup>11</sup>A. K. Turner, J. M. Woodcock, M. E. Ozsan, and J. G. Summers, *Proceedings of the 10th European Photovoltaic Solar Energy Conference, Lisbon* (Kluwer Academic, Dordrecht, 1991), p. 791.  
<sup>12</sup>M. Born and E. Wolf, *Principles of Optics* (Pergamon, New York, 1964), p. 705.  
<sup>13</sup>I. S. Nandhakumar, T. Gabriel, X. Li, G. S. Attard, M. L. Markham, D. C. Smith, and J. J. Baumberg, *CALPHAD: Comput. Coupling Phase Diagrams Thermochem.* **12**, 1374 (2004).  
<sup>14</sup>M. P. R. Panicker, M. Knaster, and F. A. Kroger, *J. Electrochem. Soc.* **125**, 566 (1978).  
<sup>15</sup>H. Yang, A. Kuperman, N. Coombs, S. MamicheAfara, and G. A. Ozin, *Nature (London)* **379**, 703 (1996).  
<sup>16</sup>H. W. Hillhouse, J. W. van Egmond, and M. Tsapatsis, *Langmuir* **15**, 4544 (1999).  
<sup>17</sup>P. Oswald, M. Moulin, P. Metz, J. C. Geminard, P. Sotta, and L. Sallen, *J. Phys. III* **3**, 1891 (1993).  
<sup>18</sup>G. W. C. Kaye and T. H. Laby, *Tables of Physical and Chemical Constants* 16th ed. (Longman, 1995), p. 1.  
<sup>19</sup>W. L. Bragg and A. B. Pippard, *Acta Crystallogr.* **6**, 865 (1953).  
<sup>20</sup>J. B. Keller, *J. Math. Phys.* **5**, 548 (1964).  
<sup>21</sup>M. V. K. Chai and S. J. Salon, *Numerical Methods in Electromagnetism* (Academic, New York, 2000).  
<sup>22</sup>M. Bonnet, *Boundary Integral Equation Methods for Solids and Fluids* (Wiley, New York, 1999).  
<sup>23</sup>M. Born and E. Wolf, *Principles of Optics*, 2nd ed. (Pergamon, New York, 1964), p. 51.  
<sup>24</sup>S. Adachi, T. Kimura, and N. Suzuki, *J. Appl. Phys.* **74**, 3435 (1993).  
<sup>25</sup>D. W. Lynch and W. R. Hunter, in *Handbook of Optical Constants of Solids*, edited by E. D. Palik (Academic, New York, 1984), p. 275.